

Research Report

Many-Particle Theory of Nuclear Systems with
Application to Neutron Star Matter

~~NGR~~ NGR -
Contract Number 19-005-006
NASA Headquarters
Washington, D. C.

Contract Number 953549
Jet Propulsion Laboratory
Pasadena, California

October 12, 1973

Signature *Dennis Chakkalakal*
Dr. Dennis A. Chakkalakal
Principal Investigator

Signature *Chia Hsing Yang*
Dr. Chia -H. Yang
Principal Investigator

Department of Physics
Southern Branch Post Office
Southern University
Baton Rouge, Louisiana 70813

MANY-PARTICLE THEORY OF NUCLEAR SYSTEMS
WITH APPLICATION TO NEUTRON STAR MATTER
(Southern Univ.) 29 p HC \$3.50 CSC 03B

63/30

Unclass
15854

N74-12479

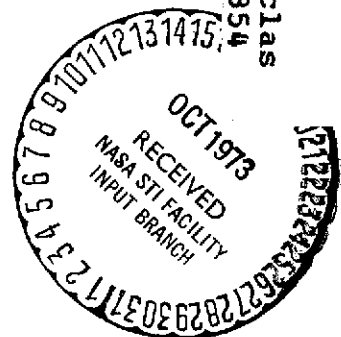


TABLE OF CONTENTS

	<u>Page</u>
In troduction	
PROJECT A	1
A-1 Constraints on Variation	1
A-2 Numerical Procedure and Results	4
A-3 Discussion	8
PROJECT B	17
B-1 Introduction	17
B-2 Polarization Effect	18
B-3 An Approximate Calculation of F_O^S	18
B-4 Effect of Polarization on Condensation Energy and Superfluid State Energy	20
B-5 Discussion	20

Many-Particle Theory of Nuclear Systems with
Application to Neutron Star Matter

This is a report on the research carried out on the following projects since submitting the semi-annual status report on April 5, 1973.

- A. Calculation of an improved energy-density relation for the normal state of neutron-star matter
- B. Calculation of the effects of superfluidity and polarization in neutron star matter

PROJECT A

The Calculation of an Improved Energy-Density Relation in Neutron Matter in the High-Density Region

A-1 Constraints on Variation

The theoretical formalism is outlined in section III.1 of the original proposal. In particular, the energy of the normal state of neutron matter, ϵ_n , is developed in a cluster series

$$\epsilon_n = \epsilon_F + \epsilon_2 + \epsilon_3 + \dots$$

In this report, we shall use ϵ_n to refer to our approximation for energy, namely, $(\epsilon_F + \epsilon_2 + \epsilon_3)$.

Reference is made in the original proposal to certain physically motivated necessary conditions on the radial distribution function. These in turn, constrain the variational parameters in the trial two-body correlation factor $f(r)$. There is also the so-called Pauli condition which restricts $f(r)$ directly. It arises from the effect of the Pauli Principle which prevents particles in the fermi sea from scattering back to the occupied states. The conditions which we use as constraints on our variational procedure are listed below:

- (I) $I_B = 0$ (Pauli Condition)
- (II) $S(k) \geq 0$
- (III) $I_C \leq 1.243$ (Coulomb Inequality)
- (IV) $\Delta N = 0$
- (V) $S(0) = 0$ (Structure-Factor Sum Rule)

where I_B , $S(k)$, I_C and ΔN are defined as follows:

$$I_B = \rho \int dr (f(r)-1) \left(1 - \frac{1}{2} l^2(k_F r)\right)$$

$$l(x) = \frac{3}{x} \left(\frac{\sin x}{x^2} - \frac{\cos x}{x} \right)$$

$$S(k) = 1 + S^{(0)}(k) + S^{(1)}(k) + \dots$$

$$S^{(0)}(k) = \rho \int dr e^{i\mathbf{k} \cdot \mathbf{r}} (g^{(0)}(r) - 1)$$

$$S^{(1)}(k) = \rho \int dr e^{i\mathbf{k} \cdot \mathbf{r}} sg^{(1)}(r)$$

$$g^{(0)}(r) = f^2(r) \left(1 - \frac{1}{2} l^2(k_F r)\right)$$

$$sg^{(1)}(r) = -\left(\frac{176}{105}\right) \pi \rho \frac{f^2(r)}{r} \int_0^\infty ds \int_{|r-s|}^{r+s} dt \, s t \, \eta(s) \cdot$$

$$\cdot \left[l^2(k_F t) - \frac{1}{2} l(k_F r) l(k_F s) l(k_F t) \right]$$

$$+ \pi \rho \frac{f^2(r)}{r} \int_0^\infty ds \int_{|r-s|}^{r+s} dt \, s t \, \eta(s) \eta(t) \cdot$$

$$\cdot \left[2 - (l^2(k_F r) + l^2(k_F s) + l^2(k_F t)) + l(k_F r) l(k_F s) l(k_F t) \right]$$

$$I_c = I_c^{(0)} + I_c^{(1)} + \dots$$

$$I_c^{(0)} = (4\pi\rho)^{2/3} \int_0^\infty dr \, r \left(1 - g^{(0)}(r)\right)$$

$$I_c^{(1)} = -(4\pi\rho)^{2/3} \int_0^\infty dr \, r \, sg^{(1)}(r)$$

$$\Delta N = \frac{1}{2} \rho \int dr (f^2(r)-1) \left(1 - \frac{1}{2} l^2(k_F r)\right)$$

We note that

$$2(\Delta N) = 1 + S^{(0)}(0)$$

Thus condition (IV) is equivalent to $S^{(0)}(0) = -1$. Condition (V) means

$$S(0) = 1 + S^{(0)}(0) + S^{(1)}(0) + \dots = 0$$

we use it in the truncated form

$$1 + S^{(0)}(0) + S^{(1)}(0) = 0$$

The origins of conditions (II) and (III) are discussed in E. Feenberg, Theory of Quantum Fluids (Academic Press, New York, 1969).

The relative order of magnitude of the terms in the cluster series for energy and all other associated cluster expansions is determined by the "correlation parameter" ξ defined by

$$\xi = n\omega, \quad \omega = \int (f^2(r) - 1) d\mathbf{r}$$

We note also that the five conditions are not completely independent of each other because of the following relations: Condition (V) is related to the $k = 0$ version of (II). The former can be satisfied by first satisfying (IV) and then requiring also that $S^{(1)}(0) = 0$.

In order to expedite the numerical calculation, we usually avoid imposing (II) and (III) directly. Often we find that (V) enables us to find more easily the region of the parameter space where (II) and (III) are satisfied. Similarly, (IV) (or (I)) enables us to locate regions where $|\xi|$ is small,

A-2 Numerical Procedure and Results

Several methods of calculation, each involving a different set of criteria governing the choice of constraints in the variational procedure, have been pursued. As indicated in the proposal, we have used one-parameter, two-parameter and three-parameter forms for the trial two-body correlation factor $f(r)$. Calculations using the various methods of approximation have been carried out at the density corresponding to fermi wave number, $k_F = 3.5 \text{ fm}^{-1}$ in order to test the reliability of these methods in the high-density region. The two-nucleon potential used for the purpose is the hard-core potential of core radius 0.4 fm given by Ohmura, Morita and Yamada (omy-4) (Progr. Theoret. Phys. 15 (1956) 222). This is a central potential of the form

$$V(r_{12}) = \sum_{i=1}^4 \Lambda_i V_i(r_{12})$$

$$\Lambda_1 = \Lambda_2 = \frac{1 - \vec{\sigma}_1 \cdot \vec{\sigma}_2}{4} ; \quad \Lambda_3 = \Lambda_4 = \frac{3 + \vec{\sigma}_1 \cdot \vec{\sigma}_2}{4}$$

$$V_i(r_{12}) = \begin{cases} \infty & , r_{12} < r_c \\ V_{oi} e^{-\beta_i(r_{12} - r_c)} & , r_{12} > r_c \end{cases}$$

where $i = 1, 2, 3, 4$ denotes, respectively, the component appropriate to the singlet-odd, singlet-even, triplet-even, and triplet-odd state of the two-nucleon system. The Λ_i are the corresponding projection operators. The parameters are

$$V_{02} = -235.41 \text{ MeV}, \quad \beta_2 = 2.0344 \text{ fm}^{-1}$$

$$V_{03} = -475.04 \text{ MeV}, \quad \beta_3 = 2.5214 \text{ fm}^{-1}$$

$$V_{01} = V_{04} = 0$$

$$r_c = 0.4 \text{ fm (in all States)}$$

These parameters are chosen to fit the following data characterizing the low-energy interaction of two nucleons in free space:

$$\text{Binding energy of the deuteron} = 2.226 \text{ MeV}$$

$$\text{Triplet scattering length of the neutron-proton system} = 5.378 \times 10^{-13} \text{ cm}$$

$$\text{Singlet scattering length of the neutron-proton system} = -23.69 \times 10^{-13} \text{ cm}$$

$$\text{Singlet effective range of the neutron-proton system} = 2.7 \times 10^{-13} \text{ cm}$$

A two-nucleon state must be either singlet-even or triplet-odd

according to the Pauli Principle. Therefore, in our calculation, there is no need for (V_{03}, β_3) .

Method 1

A trial two-body correlation factor,

$$f(r) = \begin{cases} 0 & , r \leq r_c \\ 1 - e^{-\mu(r-r_c)} & , r > r_c \end{cases}$$

has been used. According to the variational principle, the minimum of E_n obtained using any trial wave function provides an upper bound to the true energy E . Therefore, at each density we minimize $(E_F + E_2)$ with respect to μ . If this minimum occurs at $\mu = \mu_0$, then $E_3(\mu_0)$ is calculated. The corresponding approximation to the energy per neutron is $E_F + E_2(\mu_0) + E_3(\mu_0)$. The results obtained by this method are given in Table A-1.

Method 2

The following two-parameter form for $f(r)$ has been used in this method:

$$f(r) = \begin{cases} 0 & , r \leq r_c \\ [1 - e^{-\mu(r-r_c)}][1 + \gamma e^{-\mu(r-r_c)}] & , r > r_c \end{cases}$$

The additional parameter gives $f(r)$ more flexibility in order to help satisfy the constraints better. Several alternate approaches in imposing these conditions have been used. These are described below:

(A) The parameter μ is fixed at $\bar{\mu} = 2.0 \text{ fm}^{-1}$. γ is varied and $(E_F + E_2)$ is found to have a minimum with respect to γ at $\gamma = \gamma_0$. Then $E_3(\bar{\mu}, \gamma_0)$ is calculated.

(B) γ is determined by condition (I). Then the minimization procedure of method 1 is attempted.

(C) The same as (B), using condition (IV) instead of condition (I).

(D) The same as (B), but using condition (V) instead of (I), followed by an attempt to use the minimization procedure of method 1.

In methods (B) and (C) neither $(E_F + E_2)$ nor $(E_F + E_2 + E_3)$ is found to have a minimum with respect to μ . Results for method 2A, 2B and 2C presented in Table A-1 are intended to illustrate the following fact: As the value of μ increases, energy gets larger and convergence of all cluster expansions improves. This causes some ambiguity regarding the determination of the minimum energy. However, the ambiguity can be removed when we impose the conditions (II) and (III) on the $E_n(\mu)$ curve. This is done in method 2D for which the complete results are given in Table A-2 for μ values in the

range $2.0 \leq \mu \leq 7.0 \text{ fm}^{-1}$. It should be pointed out here that there are two values of γ that satisfies $S(0) = 0$ in method 2D. Only the smaller of these values of γ is used for each μ , since that corresponds to lower energy and better convergence of all the cluster expansions.

Method 3

Here we adopt the following three-parameter form for $f(r)$:

$$f(r) = \begin{cases} 0 & , r \leq r_c \\ [-e^{-\mu(r-r_c)}][1 + \gamma e^{-\kappa(r-r_c)}] & , r > r_c \end{cases}$$

Several different procedures involving this $f(r)$ have been attempted. Of these, the ones that turned out to be most fruitful are described below.

- (A) For given μ and κ , γ is determined by condition (I). Then it is found that at each κ , both $(\epsilon_F + \epsilon_2)$ and ϵ_n have a minimum with respect to μ at approximately the same value of $\mu = \mu_0$. Now we bring the results for $\epsilon_n(\mu_0, \kappa)$ to better agreement with the constraints by changing γ to the lower of the two values that will make $S(0) = 0$. κ is to be determined by a further minimization of energy. The results are presented in Table A-3.
- (B) In this method, the procedure in (A) is followed upto the point of obtaining the $\epsilon_n(\mu_0, \kappa)$ results. Then κ is chosen as the value κ^0 which gives the smallest $|\epsilon_n|$. Then $\epsilon_n(\mu, \kappa^0)$ is recalculated and its minimum with respect to μ is sought. The results are given in Table A-4.
- (C) In this procedure, again we let μ and κ vary, but use condition (I) to fix $\gamma = \gamma_0$ as a function of μ and κ . Then at each trial value of μ , κ is chosen as the value κ^0 for which $|\epsilon_n|$ is smallest. The resulting data for $\epsilon_n(\mu, \kappa^0)$ and other auxiliary quantities are shown in Table A-5. The lowest

energy subject to the constraints is to be determined from this data.

(D) This procedure is the same as (C) except for the following changes: Condition (IV) is used instead of (I) to fix γ ; κ^0 is chosen corresponding to the smallest value of $|I_B|$. The results are given in Table A-6.

A-3 Discussion

The lowest energy obtained by each method is shown in Table A-7.

The criteria that are used to determine the lowest energy are the following:

(1) Whenever $\mathcal{E}_n(\mu)$ or $\mathcal{E}_F + \mathcal{E}_2(\mu)$ has a minimum with respect to μ , we choose that as the lowest value in spite of the violation of $S(0) = 0$ that is usually associated with it (but, only in the high density region). However, $S(k) \geq 0$ is satisfied for k values not near $k = 0$. This can be considered adequate because in the high-density system the larger k values are much more significant. Besides, in a convergent cluster expansion for $S(k)$,

$$S(k) = 1 + S^{(0)}(k) + S^{(1)}(k) + \dots$$

the neglected higher order terms, though expected to be small, may nevertheless be sufficient to "repair" small violations of $S(0) = 0$ and

$S(k) \geq 0$ for small k . In short, the results for energy obtained from a calculation in which all the cluster expansions converge rapidly and all the conditions are satisfied with the exception of $S(k) \geq 0$ at small k ,

may be considered reliable. (2) Even when $(\mathcal{E}_F + \mathcal{E}_2)$ or \mathcal{E}_n has no minimum with respect to μ in an unconstrained variation, it is found that conditions (II) and (III) cannot be satisfied when μ is below a particular value μ_0 .

Thus $E_{\kappa}(\rho_0)$ may be taken as the lowest energy consistent with the constraints (3). Note that condition (II) is imposed in the modified sense discussed above, except for methods 2D and 3A, where we have sought to satisfy $S(k) \geq 0$ for all k . The results from these latter two methods, when compared with results from other procedures, give us an estimate of the error we may be allowing through the violation of $S(k) \geq 0$ for small k . (4) The reliability of all our results depends on the size of $|E|$ obtained; if $|E|$ is large, adequate convergence of the cluster development is in doubt. Based on all these criteria, so far the best results are obtained from method 3D.

We are in the process of testing four additional procedures involving the three-parameter correlation factor. This is expected to be completed in about three weeks from now. Then we will adopt the most reliable of the methods we have tested and carry out the complete calculation for the entire density range $0.25 \leq k_F \leq 3.5 \text{ fm}^{-1}$. It should be emphasized here that the difficulties associated with imposing $S(k) \geq 0$ for all k do not arise in the intermediate - and low-density regions.

METHOD	ξ	μ (fm ⁻¹)	γ	$S(0)$	ΔN	I_B	I_C	E_2 (MeV)	$E_F + E_2$ (MeV)	E_3 (MeV)	E_n (MeV)
1	-3.60	4.3	0	+8.6	-1.57	-0.15	-1.18	-60.1	92.2	68.1	160.
2A	-1.30	2.0	1.20	-1.1	-0.41	-0.06	0.86	-58.9	93.4	73.9	167.
2B	0.14	2.0	1.30	-1.9	0.30	0	1.31	-57.2	94.6	76.4	171.
2B	0.10	4.0	1.53	-0.4	0.18	0	1.07	+18.7	181.	68.4	249.
2C	-0.48	2.0	1.26	-2.0	0	-0.03	1.20	-57.2	94.6	75.4	170.
2C	-0.29	4.0	1.40	-0.4	0	-0.02	1.05	+12.7	165.	72.0	237

TABLE A-1

Results from Methods 1, 2A, 2B and 2C

ξ	μ (fm ⁻¹)	γ	$S^{(0)}_0$	$S^{(1)}_0$	$S(0)$	ΔN	I_B	I_C	E_2 (MeV)	$E_F + E_2$ (MeV)	E_3 (MeV)	E_n (MeV)	$S(k) \geq 0, k > 0$ violation
-1.80	2.0	1.165	-2.31	1.37	0.06	-0.65	-0.08	0.56	-59.3	93.0	72.8	166.	$3.0 \text{ fm}^{-1} \leq k \leq ?$
-1.05	3.0	1.201	-1.66	0.67	0.01	-0.33	-0.04	0.94	-41.1	111.	75.4	187.	$5.0 \text{ fm}^{-1} \leq k \leq ?$
-0.74	4.0	1.249	-1.43	0.43	0.00	-0.21	-0.03	0.96	-4.41	148.	76.0	224.	None
-0.58	5.0	1.311	-1.31	0.31	0.00	-0.15	-0.03	0.94	+43.8	196.	77.5	274.	None
-0.47	6.0	1.389	-1.23	0.23	0.00	-0.12	-0.02	0.91	103.	255.	80.1	335.	None
-0.38	7.0	1.490	-1.17	0.17	0.00	-0.09	-0.02	0.89	175.	327.	83.6	411.	None

TABLE A-2

Results from Method 2D

ξ	μ (fm ⁻¹)	K (fm ⁻¹)	γ	$S^{(a)}(0)$	$S^{(b)}(0)$	$S(0)$	ΔN	I_B	I_C	E_2 (MeV)	$E_F + E_2$ (MeV)	E_3 (MeV)	E_n (MeV)	$S(k) \geq 0, k > 0$ Violation
-2.06	3.0	2.0	0.34	-2.54	1.53	-0.01	-0.77	-0.09	0.28	-59.6	92.7	70.6	163.	$2.7 \text{ fm}^{-1} \leq k \leq ?$
-1.21	4.0	3.0	0.52	-1.80	0.81	+0.01	-0.40	-0.05	0.89	-49.5	103.	76.5	179.	$4.0 \text{ fm}^{-1} \leq k \leq ?$
-0.83	5.0	4.0	0.68	-1.49	0.47	-0.02	-0.24	-0.04	0.96	-18.2	134.	77.6	212.	None
-0.63	6.0	5.0	0.82	-1.34	0.34	0.00	-0.17	-0.03	0.94	+26.1	178.	78.9	257.	None
-0.50	7.0	6.0	0.96	-1.25	0.25	0.00	-0.13	-0.02	0.92	83.1	235.	81.2	317.	None
-0.41	8.0	7.0	1.10	-1.19	0.19	0.00	-0.10	-0.02	0.89	152.	304.	84.7	389.	None

TABLE A-3

Results from Method 3A

ξ	μ (fm ⁻¹)	K^0 (fm ⁻¹)	γ	$S^{(0)}$	$S^{(1)}$	$S(0)$	ΔN	I_B	I_C	ϵ_2 (MeV)	$\epsilon_F + \epsilon_2$ (MeV)	ϵ_3 (mev)	ϵ_n (mev)	$S(k) \geq 0$ Satisfied for
0.17	2.5	3.2	2.62	-0.60	-0.99	-0.59	0.20	0	1.08	31.1	183.	61.4	245.	$1.2 \text{ fm}^{-1} < k < ?$
0.09	3.0	3.2	1.66	-0.60	-0.99	-0.59	0.20	0	1.15	-11.3	141.	70.0	211.	$1.8 \text{ fm}^{-1} < k < ?$
0.08	3.5	3.2	1.16	-0.58	-1.11	-0.69	0.21	0	1.17	-24.1	128.	74.2	202.	$1.6 \text{ fm}^{-1} < k < ?$
0.08	4.0	3.2	0.87	-0.58	-1.14	-0.72	0.21	0	1.18	-27.0	125.	75.1	200.	$1.6 \text{ fm}^{-1} < k < ?$
0.08	4.5	3.2	0.68	-0.58	-1.13	-0.71	0.21	0	1.18	-25.6	127.	74.9	202.	$1.6 \text{ fm}^{-1} < k < ?$
0.08	5.0	3.2	0.56	-0.59	-1.08	-0.67	0.21	0	1.17	-21.9	130.	74.5	205.	$1.6 \text{ fm}^{-1} < k < ?$

TABLE A-4

Results from Method 3B

ξ	μ (fm ⁻¹)	K^0 (fm ⁻¹)	γ	$S^{(0)}$	$S^{(1)}$	$S(0)$	ΔN	I_B	I_C	E_2 (MeV)	$E_F + E_2$ (MeV)	E_3 (MeV)	E_n (MeV)	$S(k) \geq 0$ Satisfied for
0.23	1.4	1.75	2.36	-0.36	-2.58	-1.94	0.32	0	0.81	-45.9	106.	85.5	192.	$0.4 < k < 1.2 \text{ fm}^{-1}$ $2.0 < k < 3.7 \text{ fm}^{-1}$
0.18	1.6	2.00	2.38	-0.44	-2.00	-1.44	0.28	0	1.09	-39.0	113.	80.2	193.	$0.6 < k < 1.2 \text{ fm}^{-1}$ $2.0 < k \lesssim 5.0 \text{ fm}^{-1}$
0.17	1.8	2.26	2.42	-0.49	-1.63	-1.12	0.25	0	1.14	-28.0	124.	75.6	200.	$0.7 < k < 1.3 \text{ fm}^{-1}$ $2.2 < k < ? \text{ fm}^{-1}$
0.19	2.0	2.60	2.68	-0.53	-1.37	-0.90	0.23	0	1.04	-1.27	151.	73.5	225.	$k > 0.7 \text{ fm}^{-1}$
0.16	2.2	2.80	2.55	-0.56	-1.19	-0.75	0.22	0	1.12	3.68	156.	67.4	223.	$k > 0.9 \text{ fm}^{-1}$
0.17	2.5	3.22	2.66	-0.60	-0.99	-0.59	0.20	0	1.07	34.8	187.	61.1	248.	$k > 1.0 \text{ fm}^{-1}$
0.16	2.8	3.55	2.59	-0.62	-0.86	-0.48	0.19	0	1.05	52.1	204.	56.9	261.	$k > 1.1 \text{ fm}^{-1}$
0.17	3.0	3.80	2.61	-0.63	-0.79	-0.42	0.18	0	1.03	70.6	223.	54.0	277.	$k > 1.1 \text{ fm}^{-1}$
0.17	3.2	4.04	2.62	-0.64	-0.74	-0.38	0.18	0	1.01	88.2	241.	51.7	292.	$k > 1.0 \text{ fm}^{-1}$
0.18	3.5	4.46	2.73	-0.65	-0.68	-0.33	0.17	0	0.97	128.	281.	46.3	327.	$k > 0.9 \text{ fm}^{-1}$
0.18	3.8	4.80	2.72	-0.66	-0.63	-0.29	0.17	0	0.95	155.	308.	44.4	352.	$k > 0.9 \text{ fm}^{-1}$

TABLE A-5

Results from Method 3C

ξ	μ (fm ⁻¹)	χ^0 (fm ⁻¹)	γ	$S^{(0)}(0)$	$S^{(1)}(0)$	$S(0)$	ΔN	I_B	I_c	ε_2 (MeV)	$\varepsilon_F + \varepsilon_2$ (MeV)	ε_3 (MeV)	ε_n (MeV)	$S(k) \geq 0$ Satisfied for
-0.40	1.4	1.80	2.53	-1.01	-1.77	-1.78	0	-0.03	0.69	-41.5	111.	88.7	200.	$0.4 < k < 1.3 \text{ fm}^{-1}$ $2.0 < k < 4.2 \text{ fm}^{-1}$
-0.37	1.6	2.04	2.47	-1.00	-1.32	-1.32	0	-0.02	1.13	-35.8	116.	79.7	196.	$0.7 < k < 1.3 \text{ fm}^{-1}$ $2.0 < k < ? \text{ fm}^{-1}$
-0.34	1.8	2.30	2.49	-1.00	-1.00	-1.00	0	-0.02	1.20	-25.2	127.	74.0	201.	$0.8 < k < 1.4 \text{ fm}^{-1}$ $1.9 < k < ? \text{ fm}^{-1}$
-0.30	2.0	2.60	2.62	-1.00	-0.77	-0.77	0	-0.02	1.45	-6.30	146.	69.7	216.	$k > 1.0 \text{ fm}^{-1}$
-0.27	2.2	2.88	2.67	-1.00	-0.61	-0.61	0	-0.02	1.13	11.2	164.	64.8	228.	$k > 1.1 \text{ fm}^{-1}$
-0.24	2.5	3.25	2.64	-1.00	-0.44	-0.44	0	-0.02	1.10	30.6	183.	59.1	242.	$k > 1.3 \text{ fm}^{-1}$
-0.22	2.8	3.64	2.65	-1.00	-0.33	-0.33	0	-0.01	1.05	55.3	208.	54.8	262.	$k > 1.3 \text{ fm}^{-1}$
-0.21	3.0	3.90	2.67	-1.00	-0.28	-0.28	0	-0.01	1.02	72.7	225.	52.5	278.	$k > 1.2 \text{ fm}^{-1}$
-0.18	3.2	4.25	2.83	-1.00	-0.23	-0.23	0	-0.01	0.98	108.	260.	47.3	308.	$k > 1.1 \text{ fm}^{-1}$
-0.17	3.5	4.64	2.84	-1.00	-0.18	-0.18	0	-0.01	0.96	136.	289.	45.5	334.	$k > 0.9 \text{ fm}^{-1}$
-0.16	3.8	5.06	2.90	-1.00	-0.15	-0.15	0	-0.01	0.93	172.	325.	43.8	368.	$k > 0.7 \text{ fm}^{-1}$

TABLE A-6

Results from Method 3D

METHOD	ξ	μ (fm ⁻¹)	κ (fm ⁻¹)	γ	$S_{(0)}^{(0)}$	$S_{(0)}^{(1)}$	$S_{(0)}$	ΔN	I_B	I_C	ϵ_2 (MeV)	$\epsilon_F + \epsilon_2$ (MeV)	ϵ_3 (MeV)	ϵ_π (MeV)
3D	-0.30	2.0	2.60	2.62	-1.00	-0.77	-0.77	0	-0.02	1.15	-6.30	146.	69.7	216.
3C	0.16	2.2	2.80	2.55	-0.56	-1.19	-0.75	0.22	0	1.12	3.68	156.	67.4	223.
3B	0.08	4.0	3.2	0.87	-0.58	-1.14	-0.72	0.21	0	1.18	-27.0	125.	75.1	200.
3A	-0.83	5.0	4.0	0.68	-1.49	0.47	-0.02	-0.24	-0.04	0.96	-18.2	134.	77.6	212.
2D	-0.74	4.0	4.0	1.249	-1.43	0.43	0.00	-0.21	-0.03	0.96	-4.41	148.	76.0	224.

TABLE A-7

Comparison of Results from Different Methods

PROJECT B

Effects of Polarization on Neutron Star Structure

B-1 Introduction

The invisible components in the so called "single-line spectroscopic binaries" in Hercules, Scorpius, etc., seen by the UHURU satellite⁽¹⁾, are now commonly believed to be rotating neutron stars and in some cases may be even black hole revolving around the center of mass of the system. It is possible to estimate the mass of the neutron star component by an elaborate study of the intensity curves and of the spectral class of the visible components. Hence theoretical determinations of masses, moments of inertia and radii of stable neutron stars have become more important than ever.

Macroscopic neutron star properties have been calculated during the past fifteen years using equations of state derived from different phenomenological two-body interactions. One of the realistic effective interactions between two neutrons is a combination of a strong short-range repulsion and a long range attraction. It was first suggested by Migdal and later proved by Yang and Clark⁽²⁾ and others, that in a comparatively low-density degenerate neutron liquid, for which the interparticle spacing is large compared to the range of the repulsive forces (10^{-13} cm), the attraction between pairs of neutrons of opposite spin and momentum would lead to the formation of a condensate and the appearance of superfluidity. However, our estimation of the pairing energy for "S" wave attraction is on the low side, since the enhancement of the attractive interaction between neutrons arising from the fact that they are embedded in a highly polarizable medium (the other neutrons) were not taken into account by us. (Yang and Clark).

B-2 Polarization Effect

According to Pethick and Pines⁽³⁾, the additional term coming from the polarizability of the medium is always attractive and is approximately $- |VF_0^S|/(1 + F_0^S)$ where V is the "bare" interaction in the "S" wave channel and F_0^S is the Fermi liquid parameter which describes the spin-symmetric part of the interaction between two quasi-particles on the neutron Fermi surface. The net effective interaction, hence, has the simple form

$$V_{eff} = V / (1 + F_0^S) \quad (B-1)$$

Since F_0^S for the neutron liquid is negative and according to Pethick & Pines may be as negative as -0.7, such enhancement effects can be very important. An exact estimation of F_0^S seems unattainable at present although such a calculation is desirable and necessary in order to understand exactly how the polarized medium affects the energy state and therefore the mass-energy density inside the neutron-star matter.

B-3 An Approximate Calculation of F_0^S

Applying the Landau technique of functional differentiation of the energy with respect to quasiparticle occupation numbers⁽⁴⁾, we estimate the Fermi liquid parameter F_0^S by summing over both the direct and exchange interactions between the interacting quasiparticle pair via the following integral

$$F_0^S = \frac{N_0}{2} \frac{(2\pi)^3}{\Omega} \int_0^{2k_F} \frac{k dk}{k_F^2} [V(0) - V(k)] \quad (B-2)$$

Where $N_0 = m^*k_F/2\pi\hbar^2$ is the familiar density of states at the Fermi surface, and Ω is the volume of the system.

For the interaction between a quasiparticle pair, we choose the simple Yamaguchi potential⁽⁵⁾

$$(k'|V|k) = -(\hbar^2/m) K g(k') g(k), \text{ (S-wave only)} \quad (\text{B-3})$$

with $g(k) = (\beta^2 + k^2)^{-1}$. For $K = 0.18725 \text{ fm}^{-3}$ and $\beta = 1.254 \text{ fm}^{-1}$ the singlet scattering length and effective range are $a_s = -23.75 \text{ fm}$ and $r_s = 2.490 \text{ fm}$.

The Fermi liquid parameter F_O^S is calculated for several densities. The results are listed in Table B-1

Table B-1 F_O^S for different densities

$k_f(\text{fm}^{-1})$	0.46	0.60	0.72	0.96	1.20
F_O^S	-0.081	-0.262	-0.364	-0.552	-0.734

As can be seen from Table B-1, F_O^S depends on density quite strongly. As the density increases, the F_O^S becomes more and more negative. At the density $k_f = 1.20 \text{ fm}^{-1}$, F_O^S is equal to -0.73. These results together with the prediction by Pethick and Pines give a very strong indication that the enhancement due to the polarization of the neutron medium may even be large enough to give rise to a major mass-energy density discontinuity due to neutron pairing effects. The existence of a concavity in the mass-energy density vs. the number density curve is sufficient to give a first-order phase-transition. Since there is no precise way of calculating the energy state for the neutron-star matter including the polarization effect, it is of interest to see how strong the enhancement will have to be in order to produce a first-order phase-transition.

B-4 Effect of Polarization on Condensation Energy and Superfluid-State Energy

As has been mentioned in our original proposal we have all the necessary ingredients for the calculation of the normal state energy, \mathcal{E}_n , and the condensation energy, \mathcal{E}_c , and also the superfluid state energy, $\mathcal{E}_s (= \mathcal{E}_n - \mathcal{E}_c)$. To simplify the calculation, we assume that the enhancement due to polarization results in an increase in the attractive potential well-depth only. Then all we have to do in the calculations of the enhanced normal state energy, $\mathcal{E}_n^{\text{enh}}$, and the enhanced condensation energy, $\mathcal{E}_c^{\text{enh}}$, is to substitute A_0 by βA_0 ($\beta > 1$) in the Ohmura potential⁽⁶⁾

$$V(12) = \begin{cases} \infty & , & r_{12} < c \\ A_0 \exp(-\alpha r) & , & \text{S-wave only, } r_{12} > c \end{cases} \quad (\text{B-4})$$

Where c is the radius of the hard core. $\mathcal{E}_n^{\text{enh}}$, $\mathcal{E}_c^{\text{enh}}$ and $\mathcal{E}_s^{\text{enh}}$ ($= \mathcal{E}_n^{\text{enh}} - \mathcal{E}_c^{\text{enh}}$) are then calculated according to the procedures described in our proposal for the $c = 0.4$ fm Ohmura potential. The results of $\mathcal{E}_n^{\text{enh}}$, $\mathcal{E}_c^{\text{enh}}$, and $\mathcal{E}_s^{\text{enh}}$ for $\beta = 1.0, 1.30, 1.45$, and 1.50 are listed in Table B-2. (Note that a $\beta = 1.50$ is corresponding to a $F_0^S = -0.33$.) For the purpose of easier reference, we show in Figure B-1 the plots of the enhanced normal state energy per particle vs. k_f for $\beta = 1.0, 1.15, 1.30, 1.45, 1.50, 1.55, 1.60$, and 1.80 . In Figure B-2, the enhanced superfluid state energy per particle $\mathcal{E}_s^{\text{enh}}$, vs k_f for $\beta = 1.30, 1.45$, and 1.50 are plotted. Some interesting sets of energies in Figure B-1 are plotted vs. the specific volume, ν , in Figure B-3.

B-5 Discussion

From Table B-2 and Figure B-2 we find that at $\beta = 1.45$, the superfluid state energy, $\mathcal{E}_s^{\text{enh}}$, turns negative at $k_f = 0.5 \text{ fm}^{-1}$, while at $\beta = 1.50$, $\mathcal{E}_s^{\text{enh}}$ turns

negative at $k_f = 0.65 \text{ fm}^{-1}$ resulting in a major mass-energy density discontinuity around the density 10^{12} - $10^{13} \text{ gm-cm}^{-3}$.

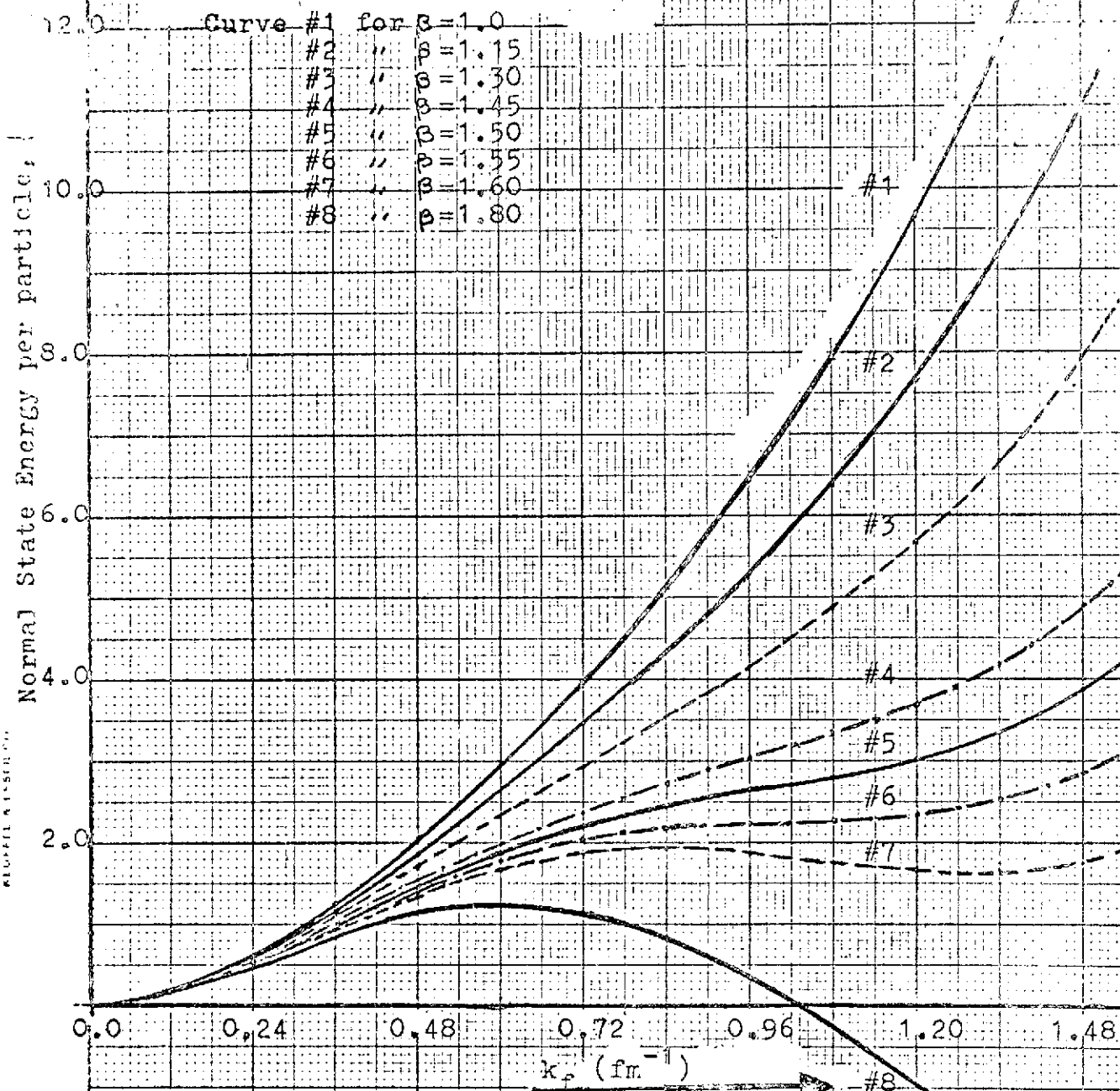
We conclude that the polarization effect indeed enhances the condensation energy (and the gap) and there is a tendency of the neutron-star matter to undergo a first-order phase-transition around the density of 10^{12} - $10^{13} \text{ gm-cm}^{-3}$ provided the effect is as strong as indicated (or stronger).

References

1. R. Giacconi, S. Murray, H. Gursky, E. Kellogg, E. Schrier and H. Tanenbaum, *Astrophys. J.*, 178 (72) 281
2. C. -H. Yang and J. W. Clark, *Nucl. Phys.* A174 (71) 49
J. W. Clark and C. -H. Yang, *Nuovo Cimo Lett.* 1(1970) 272, 2(1971) 379
3. D. Pines in *Proc. XIIth Into Conf. Low. Temp. Phys.*, edited by E. Kandu Tokyo, 1971
4. G. E. Brown, *Rev. of Modern Phys.* 43 (1971) 1
5. Y. Yamaguchi, *Phys. Rev.*, 95 (1954) 1678
6. T. Ohmura, *Progr. Theo. Phys.* 41 (1969) 419

Table B-2 Condensation energy, \mathcal{E}_c , normal state energy per particle, and superfluid state energy per particle for $\beta = 1.0$ (unenhanced), 1.30, 1.45, and 1.50 (enhanced)

β	$k_f(\text{fm}^{-1})$	n (MeV)	c (MeV)	s (MeV)
1.0	0.24	0.606	0.114	0.492
	0.48	2.050	0.294	1.756
	0.60	2.960	0.301	2.659
	0.72	3.990	0.220	3.770
	0.84	5.150	0.131	5.019
	1.08	7.935	0.012	7.923
	1.20	9.655	0.001	9.654
1.30	0.36	1.103	0.436	0.667
	0.48	1.705	0.773	0.932
	0.60	2.319	1.120	1.199
	0.72	2.925	1.030	1.895
	0.84	3.527	0.765	2.762
	0.96	4.155	0.504	3.651
	1.08	4.853	0.352	4.501
	1.20	5.674	0.107	5.567
	1.32	6.679	0.021	6.658
1.45	0.36	1.028	1.065	-0.037
	0.48	1.533	1.601	-0.068
	0.60	1.996	1.777	0.219
	0.72	2.390	1.685	0.705
	0.84	2.719	1.331	1.388
	0.96	3.012	0.933	2.079
	1.08	3.315	0.564	2.751
	1.20	3.686	0.277	3.409
	1.32	4.189	0.051	4.138
1.50	0.36	1.003	1.270	-0.267
	0.48	1.476	1.853	-0.377
	0.60	1.888	2.070	-0.182
	0.72	2.212	1.959	0.253
	0.84	2.450	1.554	0.896
	0.96	2.632	1.105	1.527
	1.08	2.803	0.686	2.117
	1.20	3.023	0.359	2.664
	1.32	3.359	0.068	3.291

$$c = 0.4 \text{ f m}$$
$$|A_0| = 235.414 \text{ MeV}$$
$$\alpha = 2.0344 \text{ fm}^{-1}$$


Parameters for the potential used

$$c = 0.4 \text{ fm}$$

$$A_0 = 235.414 \text{ MeV}$$

$$\alpha = 2.0344 \text{ fm}^{-1}$$

Curve #1 for $\beta = 1.30$

#2 " $\beta = 1.45$

#3 " $\beta = 1.50$

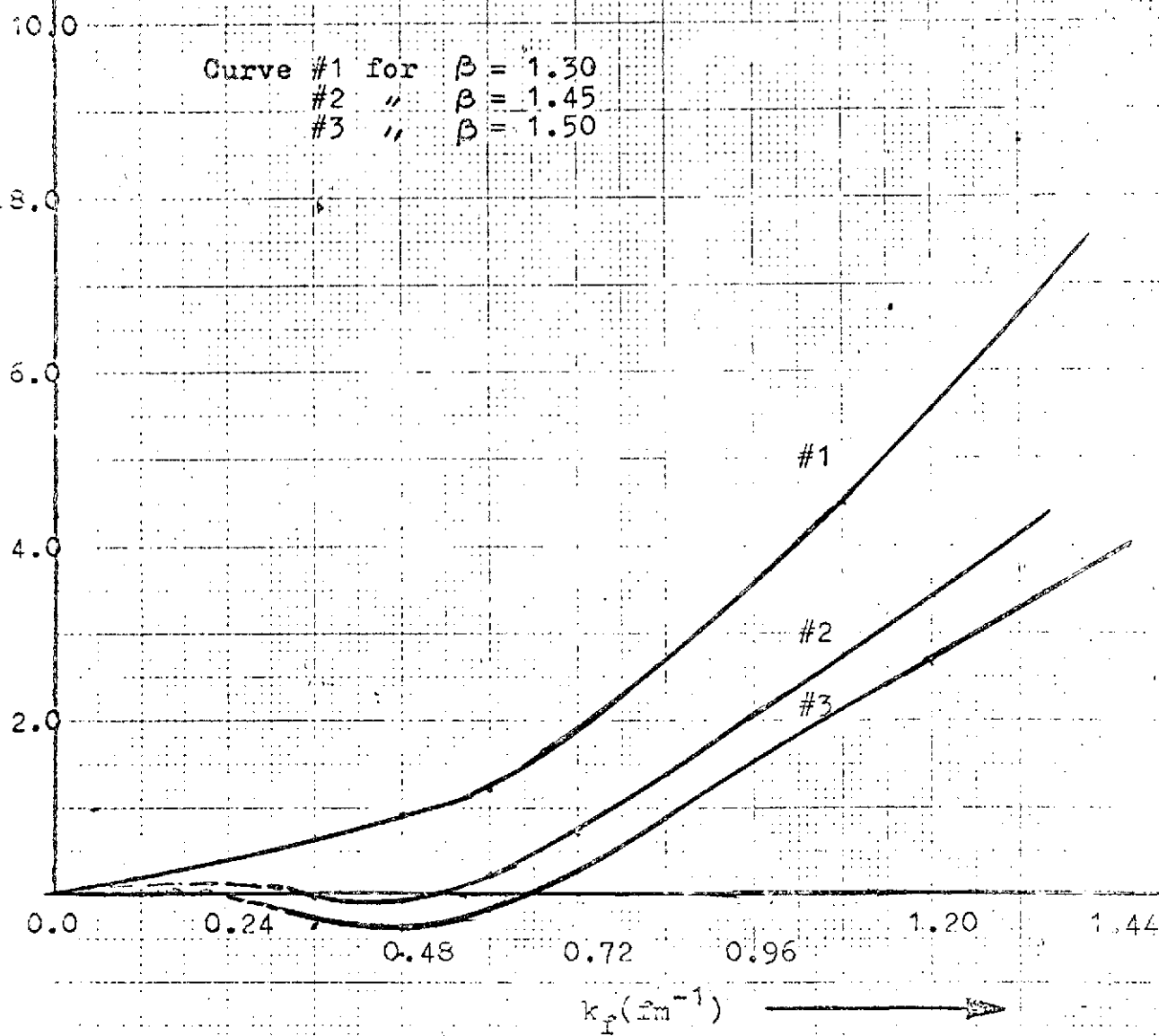


Figure B-2

